Extended Abstracts of the 2018 International Conference on Solid State Devices and Materials, Tokyo, 2018, pp1175-1176

Mo2C/MoS2 Lateral Heterostructure formed by Chemical Conversion of Molybdenum Disulfide

Seunghyuk Choi[1], Jaeho Jeon[1], Young Jae Song[1], Jeong Ho Cho[1], Sungjoo Lee[1*]

[1] SKKU Advanced Institute of Nanotechnology (SAINT), Sungkyunkwan University
Suwon 440-746
Phone: +82-5583-4667 E-mail: huk9022@gmail.com, *leesj@skku.edu

Abstract

The metallic molybdenum carbide (Mo_2C) which is one of the MXene was synthesized through the chemical conversion of semiconducting molybdenum disulfide (MoS_2). The conversion area of Mo_2C was controlled by that adjusting the thermal annealing time under the CH_4 and H_2 atmosphere. The metallic Mo_2C film was synthesized with a sheet resistance of 123.6 Ω sq^{-1}. Atomically sharp Mo_2C/MoS_2 lateral junction were formed with low contact resistance (1.2 kΩ·μm) and low Schottky barrier height (26 meV). This work provides a manufacturable synthesis method of Mo_2C from MoS_2 and the formation of a metal/semiconductor in-plane junction structure. This brand-new synthesis strategy of MXene will be a greatly important for future 2D heterojunction structures and feasible device applications.

1. Introduction

Mxenes, which are one of the group of two-dimensional (2D) materials, have attracted great interest in recent years as part of efforts to investigate 2D materials beyond graphene. The attractive properties of MXenes have been reported such as an ultrahigh electrical conductivity (Mo_2C) [1], an excellent thermal conductivity (Ti_2CO_2) [2], and unique optoelectronic activities (Ti_2CT_x) [3,4], which overcome several fundamental limits of other 2D Materials. In spite of the demonstrated excellent properties of MXenes, applications of MXenes have been limited by a lack of scalable synthesis methods that yield stable MXene films. In this work, we demonstrated that the synthesis of the fully converted 2D metallic Mo_2C layers through the chemical conversion process of 2D MoS_2 crystals with the thermal annealing under CH_4 and H_2, using Cu foil as a catalyst. The converted Mo_2C region was determined by thermal annealing time period. The electronic properties of the synthesized Mo_2C were investigated through the four-probe and Hall measurements. Fully converted Mo_2C nanosheets measured an excellent sheet resistance (123.6 Ω sq^{-1}) and carrier concentration (5.84×10^{-13} cm^{-2}). Partial conversion of MoS_2 by controlling the annealing period provided the formation of metallic/semiconducting (Mo_2C/MoS_2) junction with an atomically sharp interface and a low contact resistance (1.2 kΩ·μm) and Schottky barrier height (SBH) (26 meV).

2. Results and discussion

Synthesis of Mo_2C nanosheets via chemical conversion process of MoS_2 .

Fig. 1 (a) describes the process by which Mo_2C nanosheets were converted from MoS_2 crystals under CH_4 and H_2 under 820 °C thermal heating. The chemical conversion of Mo_2C started, where hydrodesulfurization and carburization occurred. S atoms at the edge were separated by a reaction with H• radicals, and CH_3• radicals combined with the Mo-terminated edge (red dotted line in Fig. 1a) after decomposition of CH_4 in the existence of the Cu catalyst. The reduction of S atoms occurred proximally to the CH_3-terminated Mo, followed by the formation and lateral extension of Mo−C−Mo bonds, yielding H_2S as a byproduct. Fig. 1 (b), (c), and (d) show OM images of a single flake before (upper images) and after (bottom images) annealing under different annealing time conditions. The red dotted lines represent the area in which MoS_2 was converted into Mo_2C. The converted regions were increased as the increasing of annealing time. The Mo_2C converted region was found to increase as the thermal annealing time increased. X-ray photoelectron spectroscopy (XPS) was used to measure the chemical composition of the converted Mo_2C and the pristine and unconverted MoS_2 depending on thermal annealing time conditions. Fig. 1 (e) shows the Mo^{2+} oxidation state contributed 0% to the intensity prior to annealing, and the portion of Mo^{2+} increased to 18.27%, 37.96%, and 72.03% at 1, 2, and 3 h annealing times. This trend in the Mo 3d spectra supported the substitutional conversion from MoS_2 to Mo_2C. The atomic structure of synthesized Mo_2C/MoS_2 junction and Mo_2C nanosheets were characterized by high-resolution transmission electron microscopy (HRTEM) in Fig. 1 (f) and (g) respectively. Fig. 1 (f) shows the cross-sectional HRTEM images of the Mo_2C/MoS_2 junction. In the MoS_2 region, the layer-by-layer distance was estimated to be 6.2 Å, whereas the region in Mo_2C displayed different crystalline structures with a 1.8 Å d-spacing value along the Mo_2C (102) direction. The Mo_2C/MoS_2 heterostructure was epitaxially formed with atomically sharp interface. From Fig. 1 (g), HRTEM image with the corresponding side-view FFT pattern (inset in Fig. 1 (g)), identifying the layered structure of the synthesized Mo_2C with an atomic spacing of 4.8 Å which is correspond to the lattice parameter reported for Mo_2C in the *c* direction[5].

Electrical properties of the synthesized Mo_2C nanosheet and the Mo_2C/MoS_2 junction

The carrier transport properties of the synthesized Mo_2C nanosheets were measured using four-probe and Hall measurements, as shown Fig. 2 (a) and (b). Fig. 2 (a) shows the I –V characteristics obtained from 4-probe measurement. The Sheet resistance of Mo_2C (R_{Mo2C}) was calculated as 123.6 Ω sq^{-1} through the expression of $R_{Mo2C} = (V_{23}/I_{14}) \times (W/L)$. Fig. 2 (b) shows the carrier concentration of the synthesized Mo_2C nanosheet was extracted to be $5.84\times10^{13} cm^{-2}$ by the Hall measurement, which value was extracted from the slope of the V_H (Hall voltage) – B (magnetic field) curve. Fig. 3 (a) compares the I_D - V_G transfer curves of MoS_2 FET. Case A (red curves) shows electrons injected from Mo_2C electrode into MoS_2 channel and black curves were measured injected from Ti electrode to the MoS_2. The on-state-current from the lateral contacted Mo_2C electrode was 4 times higher than vertical contacted Ti electrode. The SBH in the lateral Mo_2C/MoS_2 junction was calculated to be 26 meV in Fig. 3 (b). From the Fig. 3 (c), We estimated the contact resistance (R_c) in the lateral MoS_2/Mo_2C junction using gate bias-induced four-probe measurements. Extremely low R_c values (20 to 1.2 kΩ·μm with $R_{channel}$ from 10^6 to 10^5 Ω sq^{-1}) were obtained from the Mo_2C/MoS_2 lateral junctions, about 2 orders of magnitude lower than the values extracted from the vertical Ti/MoS_2 junction.

3. Conclusions

In this report, we demonstrate the manufacturable synthesis method of metallic 2D Mo_2C nanosheets through the chemical conversion of semiconducting 2D MoS_2 films. Our results showed that Mo_2C nanosheets with controllable thickness (3-100 nm) and size of lateral dimension (100 μm). The synthesized Mo_2C showed an outstanding sheet resistance of 123.6 Ω sq^{-1} and the carrier concentration of 5.84×10^{13} cm^{-2}. Partial conversion of MoS_2 by controlling annealing time provided a lateral metallic/semiconducting junction that showed atomically sharp interface, excellent contact resistance(1.2 kΩ·μm) and low Schottky barrier height(26 meV) for future electronic device applications.

References

[1] Zha, X.-H.; Yin, J.; Zhou, Y.; Huang, Q.; Luo, K.; Lang, J.;Francisco, J. S.; He, J.; Du, S., J. Phys. Chem. C, **120** (2016), 15082−15088.

[2] Khazaei, M.; Arai, M.; Sasaki, T.; Chung, C.-Y.; Venkataramanan,N. S.; Estili, M.; Sakka, Y.; Kawazoe, Y, Adv. Funct. Mater, **23** (2013), 2185−2192.

[3] Xu, J.; Shim, J.; Park, J.-H.; Lee, S., Adv. Funct. Mater, **26** (2016), 5328−5334.

[4] Yang, Y.; Umrao, S.; Lai, S.; Lee, S., Adv. Funct. Mater, **8** (2017), 859 −865.

[5] Liu, Z.; Xu, C.; Kang, N.; Wang, L.; Jiang, Y.; Du, J.; Liu, Y.; Ma, X.-L.; Cheng, H.-M ; Ren, W., Nano Lett, **16** (2016), 4243−4250.

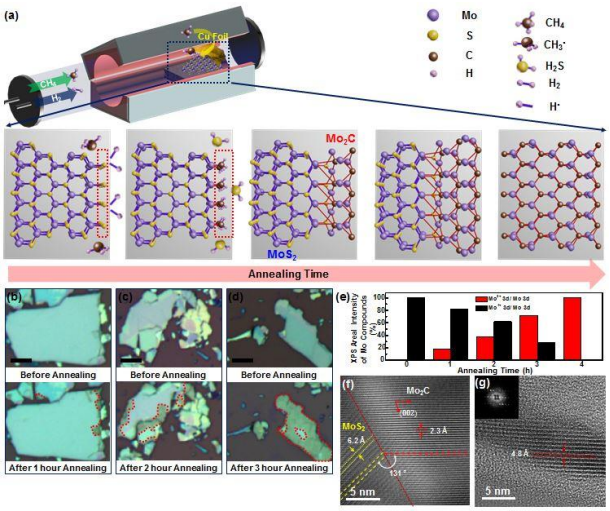

Fig. 1 (a) Schematic illustration of the Mo_2C synthesis via thermal annealing under CH_4 and H_2. (b)-(d) OM images before (upper images) and after (bottom images) annealing over different annealing times: (b) 1 h annealing, (c) 2 h annealing, and (d) 3 h annealing (Scale bars: 10μm), (e) Statistical analysis of the Mo_2C/MoS_2 XPS data to obtain the Mo^{4+} 3d and Mo^{2+} 3d XPS peak integrated intensity percentages of the Mo 3d total intensity (f) Cross-sectional view HRTEM image of the Mo_2C/MoS_2 junction (g) Cross-sectional view HRTEM image of the fully converted Mo_2C.

Fig. 2 (a) Voltage−current curves obtained from the four-terminal

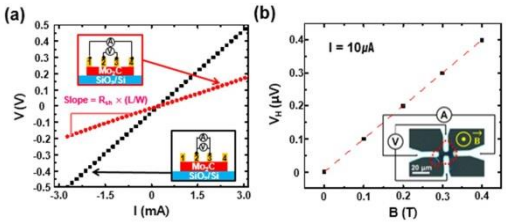

Mo_2C device and inset figure of the device structure used in each measurement (b) Hall voltage measurements under various magnetic fields and OM images of the fully converted Mo_2C device with four-terminal electrodes (inset).

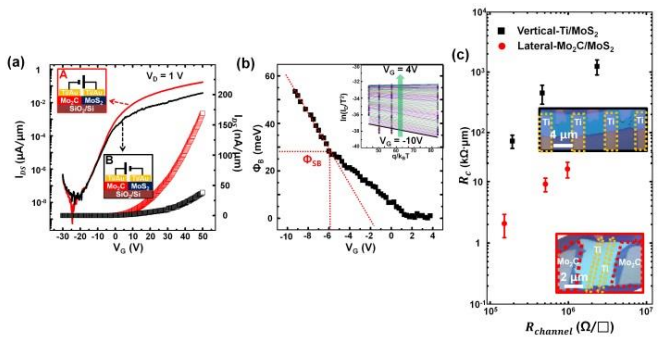

Fig. 3 (a) I_{DS} - V_G curves obtained from electrons injected from Mo_2C into MoS_2 (case A) and electrons injected from Ti into MoS_2 (case B) (b) Electron barrier heights extracted from $\ln(I_{DS}^2/T)-q/K_bT$ for a lateral Mo_2C/MoS_2 contact (c) R_c obtained using the four-probe measurement method for vertical Ti/MoS_2 contact (black rectangles) and lateral Mo_2C/MoS_2 contact (red circles).